POAC'13
Espoo, Finland

Proceedings of the 22nd International Conference on
Port and Ocean Engineering under Arctic Conditions
June 9-13, 2013
Espoo, Finland

ANALYSIS OF THE KEY PARAMETERS IN ICE INDUCED FREQUENCY LOCK-IN

Fengwei Guo [1]

[1]Det Norske Veritas AS, Høvik, Norway

ABSTRACT

In ISO 19906, the saw-tooth load function is proposed to predict the ice induced frequency lock-in vibration mode (abbreviated as FLI in this paper) on fixed vertical structures. There are still uncertainties about the parameters in the load function. The present paper attempts to perform the following analyses: 1) Relative phase analysis in time domain. This analysis takes "snapshots" along the time history, and finds out all the possible relative phases between ice load and structure's instant displacement. The intention is twofold: to identify the maximum and minimum values of relative velocity between ice edge and structure, and to develop an approximate relation between dynamic ice load amplitude and structure response; 2) Based on the presupposition that the strain rate in ice dominates the occurrence of FLI, an approximate method of estimating the highest ice velocity triggering FLI is developed; 3) Based on the hypothesis that the rate of crushing ice load is proportional to the stress rate in ice sample compression test, an approach is proposed to estimate the possible load amplitude in the saw-tooth function. Several examples are presented to validate the methods in this paper against the full scale observations.

1. INTRODUCTION

The newly published ISO 19906 standard (Petroleum and natural gas industries - Arctic offshore structures) provides extremely helpful information for the engineers who need to design structures in the ice covered waters. In spite of this, there are quite a number of remaining uncertainties in the methods proposed in the standard, and the subject of ice induced FLI (frequency lock-in) on fixed vertical structures is one typical example. FLI is a very adverse phenomenon in which the fluctuating frequency of ice load is "locked" by the structural vibration similar with resonance. Based on many full scale and model tests studying ice-structure interaction, ISO 19906 proposes: 1) A criterion to evaluate the susceptibility to FLI of a given structure; 2) An empirical equation to estimate the ice velocity which triggers FLI; 3) A time-domain ice load function which is used to analyse structure's dynamic response under FLI scenario. The methodology in ISO 19906 is based on the updated academic knowledge, but there are still uncertainties lying in several key parameters, which might confuse the designers who have limited knowledge in this field. These are discussed briefly as follows.

In ISO 19906, the basis for the criterion of susceptibility of FLI is that ice load F tends to decrease with increasing ice-structure relative velocity V_r, i.e. the negative slope in the function $F(V_r)$ (Määttänen, 1978, 1998). The main uncertainty of the criterion lies in the

empirical coefficient θ which is derived from this negative slope. A constant value is suggested for the coefficient θ in ISO 19906, and applying the criterion is found as acceptable (Guo, 2012). However, the hypothesis of the negative slope and the value of θ are still being questioned (e.g., Fransson, 2004), which remains an open topic.

The empirical equation to estimate the ice velocity causing FLI is developed according to a set of FLI events from different structures, and the maximum value of this ice velocity is believed to be proportional to structure's natural frequency (Kärnä, 2006). The prediction using this empirical equation covers all the observed ice velocities triggering FLI. However at later stage, it is found that this equation results in physically unreasonable result (Cammaert et al., 2011).

Based on the ice load time series recorded using load panels, the triangular time-domain load function is adopted in ISO 19906, which is proposed to represent the dynamic ice load which causes FLI. A few parameters are required to determine the ice load time history, in which the parameter q determines the ratio between dynamic portion of load and the maximum load. According to the rough estimation of load data, q is found in the range 0.1 to 0.5. It is stated in ISO 19906 that the maximum value q_{max} = 0.5 can be used to capture the maximum dynamic response, but there is no supportive research behind this value.

In this paper, the uncertainties mentioned above are further investigated, and the effort is made to propose approaches of estimating the key parameters better.

2. THE ICE-STRUCTURE RELATIVE VELOCITY

In this section, phase analysis in time domain is performed using the theory in structure dynamics of multi-degree-of-freedom (MDoF) system. One of the intentions is to determine the range of ice-structure relative velocity under FLI. Some of the results will be used in the later sections.

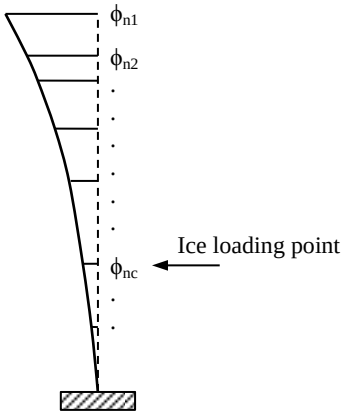

Figure.1 Multi-degree-of-freedom system of a structure with 1st order eigen mode

The MDoF system of the structure is shown in Figure.1, in which the vertical dashed line represents the structure's position without any external loading, and the solid curve shows the shape of the 1st order eigen mode. The amplitudes of the eigen mode at different elevations are denoted as ϕ_{n1}, ϕ_{n2} … etc. The dynamic equation of the structure is

$$M\ddot{X} + C\dot{X} + KX = F \tag{1}$$

According to structure dynamics, the vector of structure displacement X can be expressed by

$$X = \Phi u \tag{2}$$

In which is the matrix Φ consists of all the eigen modes, and u is a vector having the same dimension of X, and it represents the relative contribution of all the eigen modes to the total displacement X. Substituting Eq. (2) into Eq. (1), and the dynamic equation is multiplied by Φ^T, the following transformed equation is obtained.

$$M_r\ddot{u} + C_r\dot{u} + K_r u = \Phi^T F \tag{3}$$

Because of orthogonal characteristic, M_r and K_r are both diagonal matrices. Assuming that the damping matrix C_r is also in diagonal form, Eq. (1) is completely uncoupled and Eq. (3) is a series of independent equations. Ideally, it is supposed that only one eigen mode of the structure is excited (or only one eigen mode is dominant), the structure's vibration follows this eigen mode and u becomes a quantity instead of a vector. If the eigen mode is mass-normalized, and considering that the ice load only acts on the node at water level (as shown in Figure.1), the dynamic equation at ice loading point is simplified as

$$\ddot{u} + 4\pi\zeta_n f_n \dot{u} + 4\pi^2 f_n{}^2 u = \phi_{nc} F(t) \tag{4}$$

The solution of Eq. (4) is a "transformed" or so called generalized displacement u at ice loading level, and the real displacement x at ice loading level is obtained by Eq. (2). Regardless of the physical mechanism of ice load $F(t)$, the triangular saw-tooth function as proposed in ISO19906 is used as $F(t)$ (as shown in Figure.2). Substituting typical values for the parameters (e.g., damping ratio $\zeta_n = 0.005 \sim 0.05$, natural frequency $f_n = 1 \sim 5Hz$, mass-normalized eigen mode at ice loading level $\phi_{nc} = 10^{-4} \sim 10^{-3}$) into Eq.(4), the generalized displacement u can be obtained by numerical method (e.g. Newmark method). The objective of this analysis is to find out the phase shift between ice load and structure response. A typical example is shown in Figure.3.

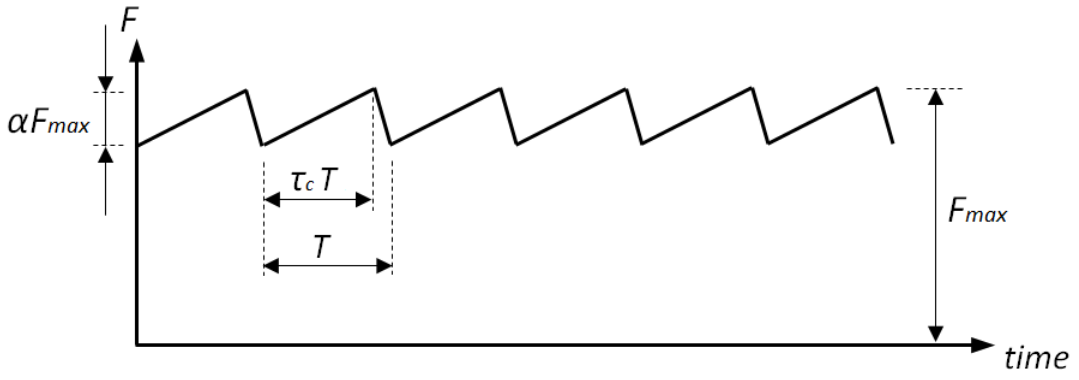

Figure.2 The saw-tooth ice load function proposed in ISO 19906 for analysing FLI

A number of numerical tests similar to Figure.3 are obtained, with changing parameters in Eq. (4). It is found that the phase shift only depends on the damping ratio ζ_n and the shape of the load time series, i.e. the parameter τ_c in Figure.2. The analysis indicates that the phase shift is close to π (i.e. half of a complete cycle) and it changes with different ζ_n and the shape factor τ_c. On the other hand, ice load measurement shows that sometimes the shape of load time

series is closer to harmonic instead of triangle. If this is the case, it is found that the phase shift in Figure.3 is close to π/2 and it changes with different ζ_n as well.

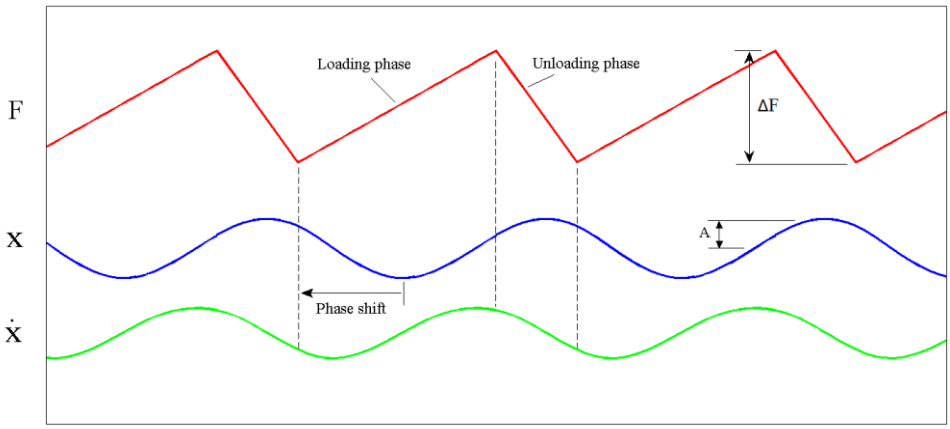

Figure.3 A typical example of the solution of Eq.(4), showing the relative phase shift between ice load and structure response ($X = \phi_{nc}\, u$)

In the example in Figure.3, the structure experiences the maximum and minimum velocity during the period of loading phase in ice load *F*. Therefore, the upper and lower bound of ice-structure relative velocity are expressed as

$$\begin{cases} V_{r,\max} = V_i + V_{str} \\ V_{r,\min} = V_i - V_{str} \end{cases} \tag{5}$$

In which V_i is the constant ice velocity, and V_{str} is the amplitude of structure velocity at ice loading level. In summary, the relative phase shift between ice load and structure response might change around the range π/2 ~ π, and the relative velocity can be in the range shown by Eq.(5) which will be used in the later section.

3. SIMPLE RELATION BETWEEN LOAD AND RESPONSE

In ISO 19906, the basis of the susceptibility of FLI is the relation between total structural damping and the "negative damping effect" caused by the ice load. From the point of energy exchange, the FLI is maintained if input energy from ice equals the energy dissipated by damping. In other words, the work done by the ice load in one complete vibration cycle is just dissipated by the damping. The numerical results in the section above are used here to analyse the energy exchange, which is discussed as follows.

Using the numerical results like the example in Figure.3, the input energy from the ice load in one complete cycle can be expressed as a function of $\Delta F \times A$. Naturally, this calculated input energy changes with different phase shifts, which are due to different load shape factors τ_c and damping ratios.

According to the transformation Eq. (2), replacing the amplitude of *X* by $A = \phi_{nc} A_u$, A_u is the amplitude of generalized displacement *u*, the input energy by ice load in one vibration cycle is $w_{in} = \lambda \phi_{nc} \Delta F A_u$. The dimensionless coefficient λ indicates the effect of different relative phase shifts. The numerical tests indicate that λ is usually higher than 1.0 and it might reach

1.6 in some cases. If the structure response is considered as harmonic approximately, i.e. $X = A\sin(\omega t)$, the energy dissipation by the damping in one vibration cycle can be estimated by integral of the work done by viscous damping force, which is expressed as:

$$w_{out} = \int_{t=0\sim T} (C\dot{X})dX \quad \Rightarrow \quad w_{out} = 8\pi^3 \zeta_n f_n^{\,2} \sqrt{1-\zeta_n^{\,2}} A_u^{\,2} \tag{6}$$

in which the interval of integral is $t = 0 \sim T$, and T is the natural period of structure considering damping effect. Because it is expected that the input and dissipated energy are the same, so that

$$8\pi^3 \zeta_n f_n^{\,2} \sqrt{1-\zeta_n^{\,2}} A_u^{\,2} = \lambda \phi_{nc} \Delta F A_u \tag{7}$$

Considering the relation between the two amplitudes

$$A = \phi_{nc} A_u \tag{8}$$

So that the amplitude of structure displacement at ice loading level under saw-tooth ice load can be approximately expressed as

$$A = \frac{\lambda \phi_{nc}^{\,2} \Delta F}{8\pi^3 \zeta_n f_n^{\,2} \sqrt{1-\zeta_n^{\,2}}} \tag{9}$$

With Eq.(9) and the maximum value λ_{max} = 1.6, the amplitude of structure displacement can be estimated. Table.1 lists a simple example of calculation, including the inputs and result.

Table.1 An example of estimating the structure response using Eq.(9)

Parameter and unit	Value
λ_{max}	1.6
ϕ_{nc}	10^{-4}
ΔF (MN)	1.0
ζ_n	0.03
f_n (Hz)	2.0
A (m)	0.05

It is noted that all the parameters in the right hand side of Eq. (9) are relatively easy to determine except ΔF, which is the critical quantity in the ice load function. An approach is proposed to estimate this parameter in the next section.

4. THE AMPLITUDE OF DYNAMIC ICE LOAD

The dynamic portion of ice load ΔF is expressed by qF_{max} in ISO 19906 or αF_{max} in Figure.2 in this paper. Given the maximum ice load F_{max} determined by the equation in ISO 19906 (or other standards), the dimensionless factor q or α will be investigated in this section.

As shown in Figure.3, one cycle of ice load variation is divided into two phases: loading phase and unloading phase. As shown in the 2D sketch of Figure.4, assuming the ice edge contacting vertical structure keeps instant without any major failure during the loading phase,

the ice edge can be approximated as a big ice sample being compressed, but naturally the compressive stress in ice is not uniformly distributed.

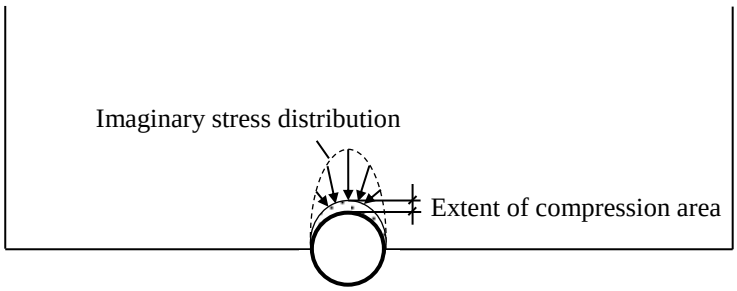

Figure.4 Sketch of ice edge contacting cylinder structure and imaginary stress distribution

It is found that the occurrence of the three ice load modes on vertical structures (intermittent crushing, FLI and continuous crushing) is dominated by the strain rate in ice, and FLI takes place when the strain rate in the range of ductile-brittle transition (Yue et al., 2009). Therefore, the dynamic portion of ice load might be estimated by the following equation.

$$\Delta F = IDh\frac{\Delta\sigma}{\Delta t}T_{loading} \tag{10}$$

In which D is structure diameter and h is ice thickness. $\Delta\sigma/\Delta t$ is a "representative" stress rate. Because the compressive stress is not uniformly distributed as shown in Figure.4, the term $\Delta\sigma/\Delta t$ is the maximum stress rate at the location on the symmetrical axis. $T_{loading}$ represents the duration of the loading phase, as shown in Figure.3, so that the term $(\Delta\sigma/\Delta t)\ T_{loading}$ is the stress accumulated on the symmetrical axis during the loading phase. By introducing a scaling factor I which considers the non-uniform stress distribution along the half cylinder, the stress accumulation on the structure surface is summed up to obtain ΔF as expressed in Eq.(10).

Under the presupposition that the strain rate $\dot{\varepsilon}$ in ice keeps in the range of ductile-brittle transition, and assuming the Young's modulus E keeps more or less constant during loading process, Eq.(10) can be transformed into the form of Eq.(11).

$$\Delta F = IDhE\dot{\varepsilon}T_{loading} \tag{11}$$

On the other hand, the maximum ice load acting on vertical structure can be expressed as $F_{max} = Dhp_{max}$, in which p_{max} is the nominal maximum pressure on the structure. Therefore, the ratio $\alpha = \Delta F / F_{max}$ can be expressed as Eq.(12).

$$\alpha = I\frac{E}{p_{\max}}\dot{\varepsilon}T_{loading} \tag{12}$$

The right hand side of Eq. (12) includes several parameters which can be considered as deterministic, while the others are more probabilistic. For example, the scaling factor I accounts for the non-uniform stress distribution sketched in Figure.4, although the magnitude of I is unknown, it is certainly lower than 1.0, probably around 0.5. $T_{loading}$ can be determined as a portion of the natural period of structure as shown in Figure.2, and the coefficient τ_c falls in the range of 0.5 ~ 0.9 according to ISO 19906. It is commonly known that the ductile-brittle transition range is around $\dot{\varepsilon} = 10^{-4} \sim 10^{-3} s^{-1}$ (Sanderson, 1988, Timco, 2010), which can

be used in Eq. (12). The maximum nominal pressure p_{max} includes some uncertainties, which needs to be determined by the designer, and the equation in ISO 19906 can be one option. The Young's modulus E is another probabilistic parameter with typical range of 1 ~ 3 GPa.

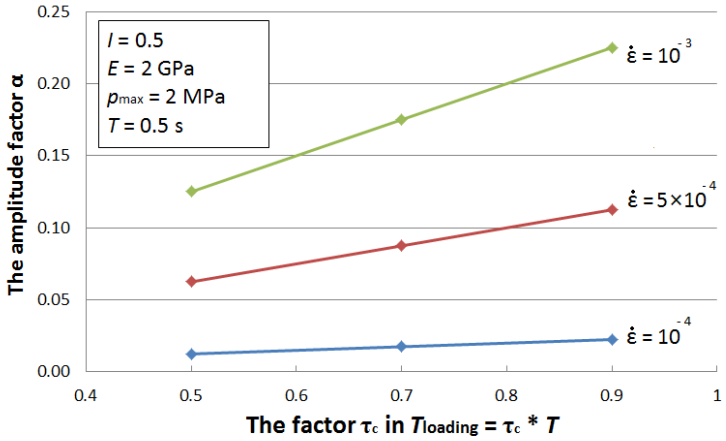

Figure.5 Examples of the ratio α calculated by Eq.(12)

Figure.5 shows a set of estimated values of the ratio α under different given inputs. As mentioned above, the Young's modulus E depends on the ice quality and p_{max} depends on ice load equation being used. These two parameters are the main uncertainties and probabilistic models should be applied on them.

5. THE ICE VELOCITY TRIGGERING FLI

The physical mechanism of FLI indicates that the different strain rate in ice dominates the three dynamic crushing load patterns (Yue et al, 2009, 2012), but strain rate is a difficult variable for the engineers to deal with. Ideally, it's better to link the strain rate to the ice velocity range which causes FLI, so the designers know what ice velocities might trigger FLI for a given structure. According to field observation, crushing ice load appears intermittent pattern under very low ice velocity, and might enter the dangerous FLI zone when the ice velocity increases, finally, the FLI can't be maintained when ice velocity becomes higher, which is continuous crushing. The key question is: what is the highest ice velocity which is able to cause FLI.

Kärnä (1990, 2001) developed a model to predict this "boundary" between FLI and continuous crushing. ISO 19906 adopted the methodology by Kärnä (2006) and proposes that this "boundary" velocity is proportional to structure's natural frequency. This linear relation is based on the fitting of the data events from 14 different tests, which are reported as FLI scenarios. The relation in ISO 19906 provides acceptable result if the structure's fundamental natural frequency is lower than 5 Hz, however, it is found later that this empirical relation results in physically incorrect conclusion (Cammaert, et al., 2011). In other words, the relation is not generic.

In this section, the effort is made to develop a generic criterion to estimate the highest ice velocity triggering FLI, and the starting point is the physical mechanism of FLI. According to the physical mechanism, FLI is achieved only if the strain rate in ice keeps within ductile-brittle transition zone during the loading phase of ice load (Yue et al, 2012). In other words,

the monotonous increasing during loading phase will collapse if the strain rate becomes too high which results in brittle failure of ice.

The relation between strain rate in ice and other variables has been studied since 1970's (e.g. Michel et al., 1977, Ralston, 1979, Palmer et al., 1983). Due to the complex 3D indentation between vertical structure and thick ice, strain rate is believed as a function of relative velocity V_r, structure width D and ice thickness h. Obviously, the strain rate is spatially dependent, and it drops down rapidly at the locations a little far away from the ice-structure interaction surface. Despite the spatial difference of strain rate, most of the previous research tried to use the variables (e.g. V_r, D, h) to predict an effective or a "representative" strain rate, which is at the same magnitude order as the maximum strain rate on the ice-structure interaction surface. This is because it is the strain rate in the thin ice layer close to structure that dominates the loading, and the crushed thin ice layer has been observed in field test (Bjerkas, 2005).

In this paper, a simple scenario is focused in which the ice is relatively thin compared with structure width, i.e. the aspect ratio D/h is high. In this case, the structure's indentation to ice sheet can be approximated as plane stress state, and the stress or strain can be considered constant in the vertical direction along ice thickness. Therefore, the effective strain rate $\dot{\varepsilon}$ is a function of only relative velocity V_r and structure width D. There are different simple equations to express $\dot{\varepsilon}(V_r, D)$ (e.g. Michel et al., 1977, Ralston, 1979, Palmer et al., 1983), and the following equation is used in this paper.

$$\dot{\varepsilon}_{eq} = \frac{V_r}{1.8D} \tag{13}$$

The derivation of Eq. (13) is described in (Yue et al., 2012), and the basic approach is as follows: the ice sheet is simplified as a 2D linear elastic sheet, which has a pre-cut solid half-circle on the edge to represent the cylinder structure. The ice sheet is meshed with finite elements and compressed against the solid half-circle edge. This simple simulation shows that the maximum strain rate on the ice-structure contact surface is about V_r / (1.8D). Accordingly, Eq. (13) is used to estimate the effective strain rate, because the strain rate at anywhere in ice will never exceed the upper boundary of FLI if the maximum strain rate in Eq. (13) keeps under the boundary. It is emphasized that Eq. (13) might be questioned, and it is used here just to demonstrate the methodology.

As mentioned above, according to ice mechanics, the upper bound of strain rate for ductile-brittle transition zone is about 10^{-3} in the uniaxial compression condition. Naturally this upper bound might increase under the confined stress condition like ice-vertical structure indentation. On the other hand, the upper bound might change because of ice properties, e.g. if ice salinity or ice temperature becomes higher, the upper bound of strain rate might shift upwards. An arbitrary estimate of 10^{-2} is adopted in this paper, which represents the upper bound of strain rate for ductile-brittle transition zone under confined stress condition.

According to the phase analysis in time domain discussed above, the maximum and minimum relative velocity are expressed by Eq. (5). Many test results confirmed that V_{str} almost equals V_i during FLI (Kärnä, 2006), and this conclusion is also adopted in ISO 19906. Therefore, the maximum relative velocity becomes $V_{r,max} = 2\ V_i$. Substituting this expression into Eq. (13), the ice velocity is:

$$V_i = 0.9D\dot{\varepsilon}_{eq} \tag{14}$$

Finally, Eq. (14) can be used to estimate the maximum ice velocity triggering FLI, considering the arbitrarily defined upper bound $\dot{\varepsilon}_{eq} = 10^{-2}$. In order to test the applicability of Eq. (14), several full scale structures under FLI are used as comparison, and the results are listed in Table.2.

Table.2 Examples of applying Eq.(14) and comparison with field observations

Structure	D (m)	V_i (cm/s)	Comments
Norströmsgrund Lighthouse with load panels	7.5	6.75	Agrees well with Table.5 in (Kärnä, 2006)
Jacket platform The Bohai Sea	1.5	1.35	Agrees well with Table.5 in (Kärnä, 2006)
Sakhalin II platform (Clarke et al., 2005)	≈15~20	13.5~18	It is reported that the ice velocity of FLI can be much higher than the two structures above.

As shown in Table.2, although Eq.(14) provides reasonable results, the uncertainties still remain: firstly, Eq. (13) may not be valid under lower aspect ratio D/h; secondly, the effective strain rate's upper bound for ductile-brittle transition may not be 10^{-2} in the confined compression state, which needs to be investigated further. Despite these uncertainties, the simple Eq. (14) predicts the same trend found in field observations: experience from the lighthouse Norströmsgrund indicates that warmer ice (around 0ºC or even higher) is still able to cause FLI under high ice velocity (Bjerkås, 2005). The physical reason is: if the ice temperature increases, the strain rate's range for ductile-brittle transition will shift upwards, leading to higher ice velocity triggering FLI.

CONCLUSIONS AND DISCUSSIONS

The ice induced frequency lock-in vibration mode (FLI) on fixed vertical structure is a very harmful scenario. ISO 19906 proposes: 1) the criterion equations to judge the conditions of FLI occurring, 2) the ice load function in time domain to predict structure response of FLI, but there are still several obvious quantitative uncertainties in the methods. The present paper tries to develop a generic approach to reduce these uncertainties, and the intention is to link the physical mechanism of FLI to the parameters such as ice velocity, structure width, ice properties which are more familiar for the designers.

An approach is developed to estimate the highest ice velocity causing FLI, given the structure and ice properties; a simple equation is developed to estimate the structure response under FLI, given the dynamic portion of ice load; an approach is proposed to predict the possible range of dynamic ice load, given the structure and ice properties.

The methods and approaches developed in the present paper are in deterministic form, but the inherent uncertainties on ice properties still exist. These methods are proposed as the starting

point when designing a structure against FLI. Naturally, more observations from full scale conditions are helpful to validate the methods in the present paper.

REFERENCE

Bjerkås, M., Skiple, A. 2005. Occurrence of continuous and intermittent crushing during ice-structure interaction. Proceedings of 18th International conference on port and ocean engineering under Arctic conditions, vol.3, pp1131-1140.

Cammaert, A.B., Metrikine A.V., Hoving J.S. 2011. Performance of minimal offshore platforms in ice environments. Proceedings of the 21st international conference on port and ocean engineering under arctic conditions. Paper #27.

Clarke, C.S.J., Buchanan R., Efthymiou, M., Shaw, C. 2005. Structural platform solution for seismic arctic environments- Sakhalin II offshore facilities. The structural engineer, November, 2005, pp25-39.

Fransson; L. and Stenman, U. (2004). Mechanical properties of ice at Norstömsgrund, Tests 2003. EU FP5 EESD project No EVG1CT200200024: Measurements on Structures in Ice (STRICE). Deliverable D4.3.3. 30 p.

Guo F.W. 2012. Reanalysis of ice induced steady state vibration from an engineering perspective. 21st IAHR International Symposium on ice, paper #98.

ISO, 2010, ISO 19906:2010(E), Petroleum and natural gas industries — Arctic offshore structures, International Organization for Standardization, Switzerland.

Kärnä, T. and Turunen, R. A straightforward technique for analysing structural response to dynamic ice action. Proc. 9th Int. Conf. Offshore Mech. and Arctic Eng., 1990: pp 135-142.

Kärnä, T. 2001. Simplified modeling of ice-induced vibrations of offshore structures. Proc. 16th International symposium on Okhotsk Sea & Sea ice, 4-8 February, 2001. Mombetsu, Japan,pp114-122.

Kärnä, T. 2006, How to use saw-tooth force function to model self-excited vibration. Report Nro Karna-6-2006, Version 1.0

Michel,B. and Toussaint,N. 1977, Mechanism and analysis of indentation of ice plat. Journal of Glaciology, Vol.19,No.81. p285-300.

Määttänen, M. On conditions for the rise of self-excited ice-induced autonomous oscillations in slender marine pile structures. Winter navigation research board. Research report No 25. Helsinki University of Technology, May 1978. 98p.

Määttänen, M. Numerical model for ice-induced vibration load lock-in and synchronization. Proc. 14th Int. Symposium on Ice. Potsdam, NY. USA, 27-31 July 1998. Vol.2, pp923-930.

Palmer, A.C., Goodman, D,J., Ashby, M.F., Evans, A.G., Hutchinson, J.W. and Ponter, A.R.S. (1983): Fracture and its role in determining ice forces on offshore structures. Annuals of Glaciology, Vol.4, pp216-221.

Ralston, T.D. (1979): Sea ice loads. Technical seminar on Alaskan Beaufort Sea Gravel islands.

Sanderson. Ice Mechanics: Risks to Offshore Structures. London, UK: Graham & Trotman. 1988.

Timco, G.W., Weeks, W.F. 2010. A review of the engineering properties of sea ice. Cold regions science and technology, vol.60, pp107-129.

Yue, Q.J., Guo, F.W., Kärnä, T. 2009: Dynamic ice forces of slender vertical structures due to ice crushing. Cold Regions Science and Technology. Vol. 59. pp. 77-83.

Yue Q.J., Guo F.W., 2012. Physical mechanism of ice-induced self-excited vibration. Journal of engineering mechanics, Vol.138, No.7, pp784-790.